

# Temperature-dependent coupling of low frequency adsorbate vibrations to metal substrate electrons

J.P. Culver<sup>a</sup>, M. Li<sup>b</sup>, Z.-J. Sun<sup>a,b</sup>, R.M. Hochstrasser<sup>b</sup>, A.G. Yodh<sup>a</sup>

<sup>a</sup> Department of Physics, and the Laboratory for Research on the Structure of Matter, University of Pennsylvania, Philadelphia, PA 19104, USA

<sup>b</sup> Department of Chemistry, and the Laboratory for Research on the Structure of Matter, University of Pennsylvania, Philadelphia, PA 19104, USA

Received 24 July 1995

## Abstract

The vibrational response of CO on Cu(111) is examined following femtosecond visible pulse excitation of the substrate. We consider the effects of excitation pulse fluence on vibrational energy transfer between the CO low frequency frustrated translation and metal substrate electrons. The temperature dependent coupling rate is extracted from our data using a dynamical charge transfer model. A zero temperature coupling rate of  $\gamma_c^0 = 25(\pm 7)$  GHz ( $\tau_c^0 = 40(\pm 8)$  ps) is found to account for the energy transfer between the substrate electrons and the frustrated translation vibration.

## 1. Introduction

Femtosecond optical excitation of surfaces creates a unique environment for molecular adsorbates that often induces novel reactive processes. For most of these reactions it is crucial to consider adsorbate motions in the presence of hot substrate electron distributions. For example, coupling of adsorbate vibrations to bulk electron-hole pair excitations is of particular relevance to femtosecond vibrational heating [1–3]. State-resolved measurements of adsorbate vibrational energy relaxation [4–8] and final state analysis of femtosecond desorption products [9–12] are two classes of experiments that are used to elucidate the nature of energy transfer in these systems. There are few measurements however, wherein the basic temperature dependences of adsorbate-substrate energy transfer rates are directly examined. In this paper we report such a measurement. In particular we study

the temperature-dependent coupling between low frequency vibrations and metal substrate electrons.

Several theoretical and experimental studies have examined the energy relaxation of the high frequency stretch vibrational mode for CO adsorbed on metal surfaces. These studies provide convincing evidence for a dynamical charge transfer mechanism that couples adsorbate vibrations to substrate electron-hole pairs. The original description of this process due to Persson and Persson [13] involves a partially filled adsorbate orbital near the Fermi level of the substrate (Fig. 1). As the adsorbate vibrates, changes in the arrangement of charge on the adsorbate cause the energy level of the partially filled orbital to shift with respect to the substrate Fermi level. Since the vibrational and electronic degrees of freedom are not fully separable, energy flows between the adsorbate and the substrate during these nuclear motions.

The relevant energy scales in this dynamical charge

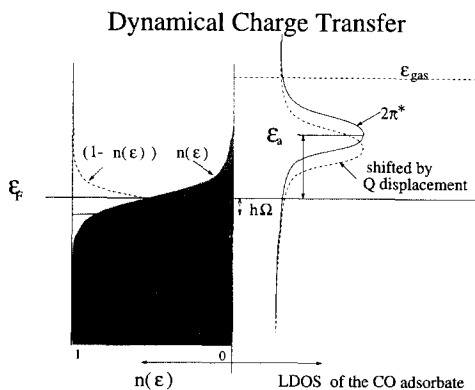


Fig. 1. The dynamical charge transfer process is illustrated by the electronic density of states for the CO/Cu(111) system. Mixing with the substrate electrons causes the  $2\pi^*$  level to lower and broaden in energy from the gas phase value. Since the amount of hybridization depends on the positions of the adsorbate nuclei, movement along a vibrational coordinate  $Q$ , will change the  $2\pi^*$  LDOS and cause charge to flow between the CO and Cu(111) substrate. The relevant energies for this process are the energy of the vibration  $\hbar\Omega$ , the thermal spread of the Fermi function ( $kT_e$ ), and the energy  $\epsilon_a$  of the  $2\pi^*$  LDOS.

transfer process are: (1) the energy of the partially filled adsorbate orbital ( $\epsilon_a$ ) relative to the metal Fermi level, (2) the energy of the vibration ( $\hbar\Omega$ ), and (3) the thermal energy of the electrons ( $kT_e$ ). Traditionally the dynamical charge transfer process has been considered in the regime where  $kT_e \ll \hbar\Omega \ll \epsilon_a$ , and has been treated as a temperature independent process [13,14]. For the CO stretch mode, a zero temperature model is thus appropriate in most situations of practical interest since  $\hbar\Omega_{\text{stretch}} (\sim 3000 \text{ K})$  is large compared to thermal energies in the calculations and compared to room temperature. There are, however, many situations in which the thermal energies in the adsorbate/substrate system become comparable with the defining energies. For example, the low frequency vibrational modes that arise when CO adsorbs on metal surfaces have energies of  $30\text{--}400 \text{ cm}^{-1}$ . The coupling of these vibrations to electron-hole pairs can be quite sensitive to the thermal distributions of the substrate electrons. In addition, intense femtosecond visible pulses can generate transient thermal electrons with temperatures of up to  $\sim 5000 \text{ K}$ . These temperatures are comparable to, or higher than, most vibrational energy levels and are within an order of magnitude of  $\epsilon_a$  for many adsorbates. Under these circumstances thermal electrons making near resonant transi-

tions can greatly enhance the energy transfer process [15].

In order to link the coupling rates obtained from low temperature measurements to highly excited non-equilibrium processes such as desorption, the basic temperature dependencies of the energy transfer process must be understood. To this end we have conducted time resolved infrared (IR) spectroscopic studies of  $(\sqrt{3} \times \sqrt{3})R30^\circ$  CO molecularly adsorbed on Cu(111) just following visible excitation pulses of differing fluences. Observations of the CO vibrational response were obtained in situ on a state specific basis, employing laser pulse excitations near the femtosecond desorption threshold. The transient vibrational dynamics of the low frequency frustrated lateral translation mode were measured. The excitation amplitude of the frustrated translation mode was monitored indirectly through its anharmonic effects on the higher frequency CO stretch mode; in particular the low frequency mode is observed to induce calculable shifts in the complex frequency of the stretch modes as its amplitude is increased. This technique has been used to study the dynamics of the frustrated translation for CO on Cu(111) [4], Cu(100) [6], and Pt(111) [5] metal surfaces. By contrast to previous studies, the analysis in this paper uses a temperature-dependent coupling rate derived from a dynamical charge transfer model for electron-hole pair coupling to adsorbate vibrations. Our new analysis provides a complete description of this temperature-dependent coupling to electrons. We find that a temperature-dependent rate, with a zero temperature value  $\gamma_e^0 = 30 \pm 7 \text{ GHz}$ , accounts for the coupling of the frustrated translation mode to the substrate electrons. In principle the couplings between adsorbate vibrations and substrate phonons are also temperature-dependent [16]. In the present experiments, however, the changes in the phonon temperature are small  $\partial T_l/T_l \sim 0.1$ . The coupling rate,  $\gamma_l$ , between the frustrated translation and the Cu phonons, is therefore taken to be temperature independent.

## 2. Description of measurement

Our experimental technique has been described in detail elsewhere [4] and is therefore only briefly outlined here. The experiment involves heating the sub-

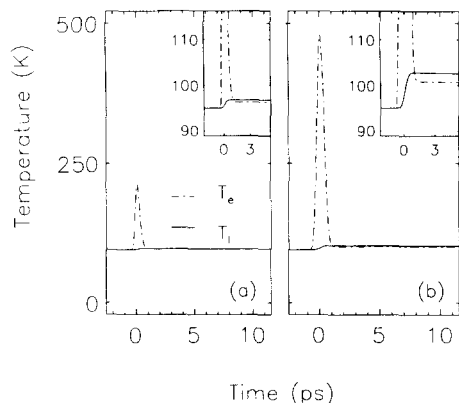


Fig. 2. The substrate temperatures,  $T_e$  and  $T_l$ , for our lowest (a), and highest (b), fluences. The energy initially deposited in the electrons creates a sharp peak in  $T_e$ . The phonons in contrast have a much larger heat capacity and therefore experience a smaller temperature rise. Since  $T_e$  is modulated much more than  $T_l$ ,  $T_e$  is more sensitive to changes in fluence. The measurements therefore probe the  $T_e$  dependence of the coupling rate between the frustrated translation and the substrate electrons.

strate with a short visible light pulse and monitoring the adsorbate response using time resolved infrared spectroscopy. Measurements were taken at various levels of substrate excitation. The visible pulse fluence was ultimately increased to a level which induced the desorption of CO.

For Cu substrates, the nascent distribution of electrons excited by direct interaction with the visible pulse thermalizes in  $\leq 70$  fs [17,18]. On longer time scales, relevant to the present experiments, the metal response is described by a model with separate electron ( $T_e$ ) and phonon ( $T_l$ ) temperatures [19,20]. These substrate reservoirs have markedly different temporal profiles that are indicated in Fig. 2 for a typical excitation pulse [21].

The CO overlayer is probed by a quasi-CW infrared pulse (30 ps) tuned near the CO stretch frequency. The reflected IR field intensity records the adsorbate susceptibility and is time-resolved by upconversion in a nonlinear crystal using a 500 fs visible gating pulse.

Although the stretch mode is nominally populated ( $< 10^{-4}$ ) through interaction with the substrate reservoirs, the dominant spectral changes observed result from a temperature dependent shift of the internal stretch complex frequency. Here the complex frequency term includes the effects of spectral shifts and damping changes. When the frustrated translation

is heated by the excited substrate, an anharmonic coupling to the stretch mode causes the internal stretch absorption to broaden and shift to lower frequency. The time-dependent population of the frustrated translation can therefore be obtained by properly interpreting the measured time evolution of the stretch mode frequency shift and broadening.

The measured signal is proportional to the imaginary component of the stretch mode polarization. Integrating the Liouville equation with a time-dependent complex stretch mode frequency yields the following expression, apart from constants, for the detected infrared field  $\mathcal{E}_{\text{gen}}(t)$  [4]:

$$\mathcal{E}_{\text{gen}}(t) = \text{Im} \left\{ i \int_{-\infty}^t dt_1 e^{-\int_{t_1}^t \Omega_{01}(\tau) d\tau} \right\}. \quad (1)$$

The complex frequency in the exponent is defined;  $\Omega_{01}(\tau) = i(\omega_L - \omega_{01}(\tau)) + \Gamma(\tau)$ , where  $\omega_L$  is the probe laser frequency,  $\omega_{01}(\tau)$  is the instantaneous stretch oscillation frequency, and  $\Gamma(\tau)$  is the instantaneous stretch dephasing rate.

The time-dependent population of the frustrated translation mode,  $n_{\text{ft}}$ , is predicted using the following rate equation for a harmonic oscillator,

$$\dot{n}_{\text{ft}} = \gamma_e(n_e - n_{\text{ft}}) + \gamma_l(n_l - n_{\text{ft}}). \quad (2)$$

where  $n_e$  and  $n_l$  represent the occupation numbers of the reservoir excitations at energy  $\hbar\Omega$  for the instantaneous temperatures  $T_e$  and  $T_l$  respectively [4].  $\gamma_e$  and  $\gamma_l$  are the coupling rates of the frustrated translation to the substrate electrons and the phonon reservoirs respectively. All previous experimental studies [4,6] used a rate equation (Eq. (2)) with *temperature-independent* values of  $\gamma_e$  and  $\gamma_l$ . *In contrast to previous studies, the present analysis utilizes a functional form for  $\gamma_e$  which depends on the instantaneous value of substrate electron reservoir temperature  $T_e$ .*

Data were taken at several frequencies for each fluence in order to increase the accuracy of the numbers reported. Some examples of the data obtained at a fluence absorbed of  $F_{\text{abs}} = 0.18$  mJ/cm<sup>2</sup> are exhibited in Fig. 3. The basic spectral feature is brought about by a shifting Lorentzian absorption profile which exhibits a maximum shift at around 2 ps and returns to an offset value within the next 10 ps. Fig. 4 exhibits data taken at five different fluences with the probe laser

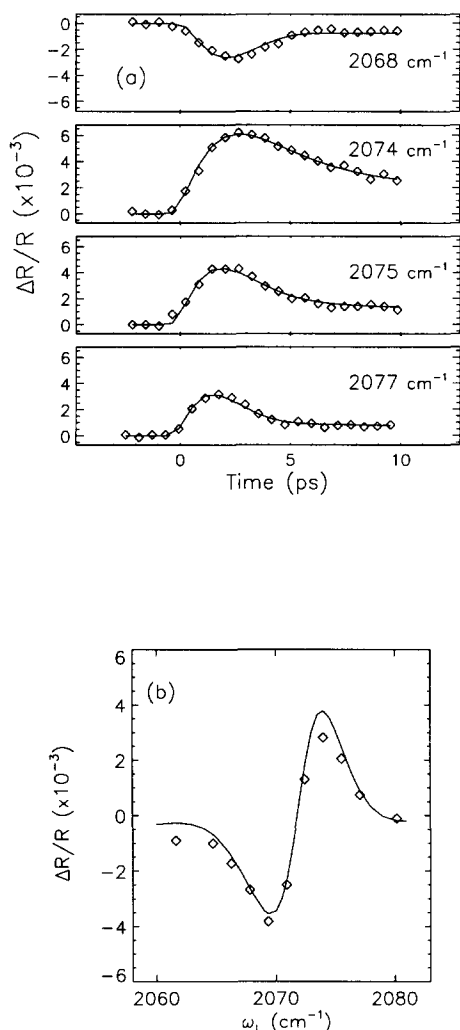


Fig. 3. Transient fractional difference reflectivity of CO on Cu(111). (a) Time scans as a function of probe laser frequency. (b) Frequency scan taken at fixed time delay of 3 ps.

tuned to  $\omega_L \sim 2074.5 \text{ cm}^{-1}$ . To maximize the signal level the low fluence measurements were taken at glancing angles ( $\theta_{\text{incident}} \sim 85^\circ$ ) where the effective CO absorption is larger. On the other hand the higher fluence data was taken at smaller incident angles to increase the fluence absorbed. When the incident angle for each measurement is taken into account the magnitude of the signal scales with the fluence absorbed. At fluences higher than  $F_{\text{abs}} = 0.33 \text{ mJ/cm}^2$  the total signal level decreased over successive time scans ( $\sim 10 \text{ min}$ ) indicating desorption of the CO. For the

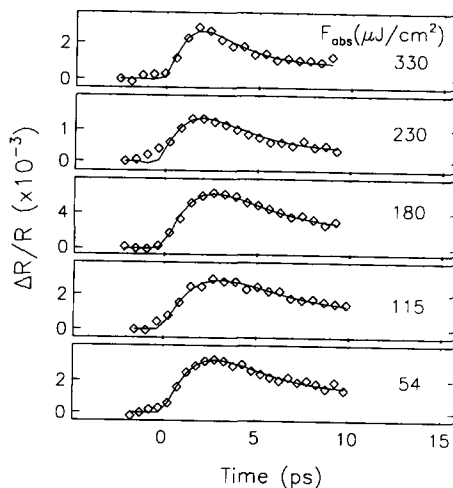


Fig. 4. Data taken at several different fluences, with  $\omega_L = 2074.5 \pm 0.5 \text{ cm}^{-1}$ . The incident angles for these measurements are:  $\theta_i = 66^\circ$  for  $F_{\text{abs}} = 330 \mu\text{J/cm}^2$  and  $F_{\text{abs}} = 230 \mu\text{J/cm}^2$ ;  $\theta_i = 79^\circ$  for  $F_{\text{abs}} = 180 \mu\text{J/cm}^2$  and  $F_{\text{abs}} = 115 \mu\text{J/cm}^2$ ;  $\theta_i = 84.5^\circ$  for  $F_{\text{abs}} = 54 \mu\text{J/cm}^2$ . The fits are described in the text.

fluences in the range of  $0.054\text{--}0.33 \text{ mJ/cm}^2$  the data clearly agree with the qualitative aspects of the time dependent exchange picture [4].

At higher fluences (see Fig. 4), there appears to be a faster adsorbate response. The faster response is due, in part, to larger net frequency shifts at higher fluences. As demonstrated in Eq. (1) the adsorbate polarization depends on the detuning between the laser frequency and the adsorbate frequency. When the probe is off-resonant the signal will oscillate at the difference frequency (i.e.  $\omega_L - \omega_{01}(\tau)$ ). The oscillations generated by the larger frequency shifts will therefore generate signals which appear to decay faster when the probe laser is tuned to the high frequency side of line center [22].

To model the temperature dependence of the coupling rate we must, in general, consider the six temperatures that are needed to describe our system: two for the substrate electrons and phonons, and four for the CO vibrational modes. In principal any of these temperatures could affect the coupling rates. However since the substrate temperatures represent thermal occupation of a continuum density of states they are the most likely to effect the coupling mechanisms. In considering the substrate temperatures, only the electron temperature varies appreciably with fluence (see Fig.

2). The change in  $T_e$  can be several times the value of the base temperature of 95 K, and the ratio of the change in  $T_e$  compared to the change in  $T_l$  is  $\delta T_e/\delta T_l \sim 20$ . Thus we concentrate on the  $T_e$  dependence of the coupling rates. The temperature dependent effects of the other reservoir coupling rates are assumed to be much smaller. We next review the dynamical charge transfer mechanisms to determine the form of a  $T_e$ -dependent coupling rate.

### 3. Temperature dependent coupling process

The basic description of electron–hole pair interaction with adsorbate vibrations was introduced by Persson and Persson [13]. It involves the flow of charge between the substrate and a partially filled adsorbate electronic state (Fig. 1). As the adsorbate is brought in contact with the metal, the normally unoccupied CO  $2\pi^*$  electronic state mixes with the substrate electrons to form hybrid states. The resulting  $2\pi^*$ -like state is shifted to energy  $\epsilon_a$  above the Fermi level, broadened, and partially occupied by the substrate electrons. This state has been observed experimentally using inverse photoemission [23] and two photon photoemission [24]. It lies 3.35 eV above the Fermi level and has a width of  $\leq 0.6$  eV.

Motion along each vibrational coordinate of the CO alters the occupancy of the  $2\pi^*$  state since the mixing depends upon the particular positions of the adsorbate nuclei. Thus, the charge transfer is dynamical. Since the electronic and vibrational degrees of freedom are not completely separable the dynamical charge transfer causes an exchange of energy between the adsorbate vibrations and the substrate electrons. An expression for the coupling rate between an adsorbate vibration and the substrate electrons ( $\gamma_e$ ) can be derived using the Andersson–Newns Hamiltonian description for the adsorbate hybridization and Fermi’s golden rule. Here we will focus on coupling to the frustrated translation vibration with coordinate  $Q$ . Employing a limited electronic basis set, the following Hamiltonian is used:

$$H = \epsilon'_a(Q) a^\dagger a + \sum_k \epsilon_k a_k^\dagger a_k + \sum_k (V_{ak}(Q) a^\dagger a_k + \text{h.c.}) + \hbar\Omega b^\dagger b, \quad (3)$$

where  $\hbar\Omega b^\dagger b$  is the energy of mode Q. The substrate electrons are described by extended wave functions ( $|k\rangle = a_k^\dagger|0\rangle$ ) with energies  $\epsilon_k$  and the adsorbate is described by an unoccupied molecular orbital ( $|a\rangle = a^\dagger|0\rangle$ ) with energy  $\epsilon'_a(Q)$  for a fixed displacement  $Q$ . The substrate  $|k\rangle$  states mix with the adsorbate state  $|a\rangle$  through the exchange terms  $V_{ak}(Q)$ . Here,  $\epsilon'_a(Q)$  is shifted from its gas phase value ( $\epsilon_{\text{gas}}$ ) as a result of all adsorbate/substrate interactions except the  $V_{ak}$  exchange terms. Expanding the energies  $\epsilon'_a(Q)$  and  $V_{ak}(Q)$  to first order in  $Q$ , the Hamiltonian can be rewritten in terms of zeroth order hybrid states  $|\alpha\rangle$  with energies  $\epsilon_\alpha$ :

$$H = \sum_\alpha \epsilon_\alpha c_\alpha^\dagger c_\alpha + \hbar\Omega b^\dagger b + H'. \quad (4)$$

The perturbation term  $H'$  represents the first order terms of the  $\epsilon'_a(Q)$ , and  $V_{ak}(Q)$  expansions, and couples the electronic ( $|\alpha\rangle$ ), and vibrational ( $|n\rangle$ ) states. For simplicity we assume that  $\partial V_{ak}/\partial Q$  is negligible and  $H'$  can be written

$$H' = \Delta_{aa} a^\dagger a (b^\dagger + b), \quad (5)$$

where

$$\Delta_{aa} = \frac{\partial \epsilon'_a}{\partial Q} \sqrt{\frac{2\hbar}{m^* \Omega}} = \frac{\partial \epsilon'_a}{\partial Q} Q_0,$$

with  $Q_0$  being the average zero temperature displacement and  $m^*$  the effective mass.

The zero temperature development of Persson [13] is now extended to non-zero temperatures by accounting for the occupied and unoccupied density of electronic states with the Fermi–Dirac distribution,  $n(\epsilon) = 1/(1 - e^{(\epsilon - \epsilon_F)/kT})$ . The mixed  $|\alpha\rangle$  states are assumed to be populated as if they are bulk metal electronic states. The energy transfer process involves a transition from vibrational state  $n = 1$  to  $n = 0$  and the scattering of an electron from an occupied hybrid state  $|\alpha\rangle$  to an unoccupied hybrid state  $|\beta\rangle$ , with  $\epsilon_\beta - \epsilon_\alpha = \hbar\Omega$ . Fermi’s golden rule yields the following expression for the coupling rate:

$$\gamma_e = \frac{2\pi}{\hbar} \sum_{\alpha\beta} |\langle \alpha, n = 1 | H' | \beta, n = 0 \rangle|^2 \times n(\epsilon_\alpha) [1 - n(\epsilon_\beta)] \delta(\epsilon_\beta - \epsilon_\alpha - \hbar\Omega), \quad (6)$$

The wave functions  $|\alpha, n\rangle$  represent the product of a hybrid state  $|\alpha\rangle$ , and a Q mode vibrational state  $|n\rangle$ .

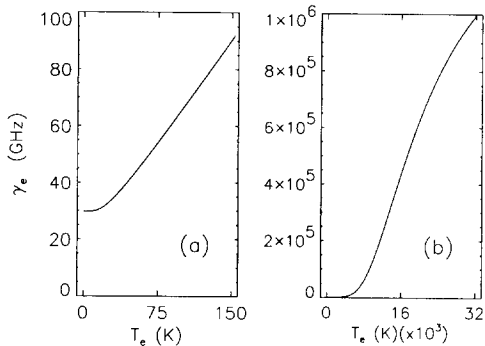


Fig. 5. Temperature dependence of  $\gamma_e$  predicted by the dynamical charge transfer model. (a) For  $T_e \ll \epsilon_a$ , (b) For  $T_e \sim \epsilon_a$ .

The coupling rate  $\gamma_e$  is rewritten in terms of the local density of states (LDOS) of the  $2\pi^*$  orbital  $\rho_a(\epsilon)$ ,

$$\gamma_e = \frac{2\pi}{\hbar} |A_{aa}|^2 \int_{-\infty}^{\infty} d\epsilon \rho_a(\epsilon) \rho_a(\epsilon + \hbar\Omega) \times n(\epsilon) [1 - n(\epsilon + \hbar\Omega)]. \quad (7)$$

For  $T = 0$  the Fermi distributions  $n(\epsilon)$ , can be replaced with step functions and Eq. (7) reduces to the result of Ref. [13]:

$$\gamma_e^0 = \frac{2\pi}{\hbar} |A_{aa}|^2 \int_{\epsilon_F - \hbar\Omega}^{\epsilon_F} d\epsilon \rho_a(\epsilon) \rho_a(\epsilon + \hbar\Omega). \quad (8)$$

However, when  $kT_e$  is comparable to, or larger than  $\hbar\Omega$ , Eq. (7) must be used.

A temperature dependence is thus introduced through the temperature dependence of the Fermi distribution. This effect can be considered in two regimes as depicted in Fig. 5. For temperatures much less than the energy of the  $2\pi^*$  level  $\epsilon_a$ , the LDOS ( $\rho_a(\epsilon)$ ) is essentially constant over the interval of integration in Eq. (7) [13,14]. The coupling rate is then expressed in terms of  $\gamma_e^0$  and a temperature factor, i.e.

$$\gamma(T_e) = \frac{\gamma_e^0}{1 - e^{-\hbar\Omega/kT_e}}. \quad (9)$$

Previously published measurements of the frustrated translation coupling rates for CO on Cu(111), Cu(100) and Pt(111) were conducted at temperatures appropriate for a coupling of this form, although this form was not employed in the analyses.

For temperatures approaching  $\epsilon_a/10$  or greater, the shape of the  $2\pi^*$  LDOS must also be included. We model the LDOS as a Lorentzian with line center 3.35 eV above  $\epsilon_F$ , and line width  $\sim 0.6$  eV [24]. Equation (7) was numerically integrated and is depicted in Fig. 5. A sharp increase in the coupling strength occurs as the substrate electrons achieve thermal energies sufficient to make near resonant transitions. For temperatures higher than  $\epsilon_a$  the resonant effect saturates and the coupling becomes less sensitive to temperature again. Similar resonance enhanced couplings have been predicted by Brandbyge et al. using a path integral technique to evaluate an electronic friction within a Langevin formalism [15]. The resulting electron temperature dependent adsorbate/substrate coupling was used to explain femtosecond laser desorption experimentals.

Both molecular orbital techniques [14,25] and density functional calculations [26] have been applied to the problem of determining the hybridization of adsorbate electronic state and the derivative of the system energy with respect to the different vibrational coordinates. With a molecular orbital calculation for copper clusters, Head-Gordon et al. [14] arrive at a temperature dependent coupling rate similar to Eq. (9). The only difference is in the calculation of  $\gamma_e^0$ . As an alternative to using Fermi's golden rule to evaluate the coupling constant, Tully et al. [16,27] have pursued molecular dynamics calculations incorporating nonadiabatic friction for the electrons. These calculations predict temperature dependent couplings to both the electron and the phonon reservoirs. The results were found to deviate from the rate equation approach in that the relaxation mechanisms to the phonons and electrons were not independent.

To use the temperature dependent coupling rate of Eq. (9) it is necessary to know the value of  $\hbar\Omega$ . Our FTIR measurements interpreted in the context of an exchange model [28,29] establish an upper limit of  $\hbar\Omega < 60 \text{ cm}^{-1}$  [4]. Additional insight into the value of  $\hbar\Omega$  is obtained by considering the experimentally determined values of the frustrated translation for atop CO on Cu(100) [6], Pt(111) [30], and Ni(111) [30]. For all of these systems the frequency lies between 30 and 60  $\text{cm}^{-1}$  and fits were carried out for  $\hbar\Omega$  values within this range.

Instead of fitting with a temperature independent rate as in previous studies, the data were fit for  $\gamma_e^0$  of

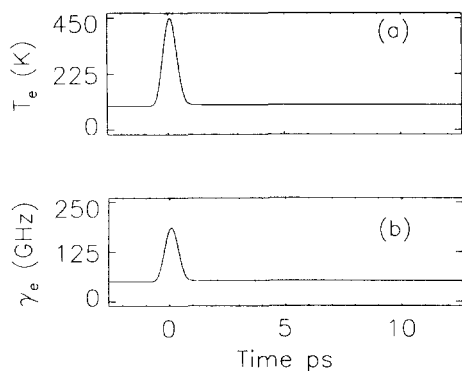


Fig. 6. The coupling rate  $\gamma_e$  depends on the Fermi distribution of the electrons. Since the electron temperature is time dependent the coupling rate is also time dependent. The time evolution of (a)  $T_e$  and (b)  $\gamma_e$  are shown for the best fit value of  $\gamma_e^0$  with  $\hbar\Omega = 45 \text{ cm}^{-1}$  and  $F_{\text{abs}} = 0.22 \text{ mJ/cm}^2$ .

Eq. (9). An intermediate value of  $\hbar\Omega = 45 \text{ cm}^{-1}$  was used to obtain the best fit value of for the zero temperature coupling rate  $\gamma_e^0 = 25(\pm 7) \text{ GHz}$ . The result was obtained using all possible light fluences. Coupling to the phonons was found to be  $\gamma_l = 280(\pm 100) \text{ GHz}$ . The fluences were fitted and determined largely by the magnitude of the signal. Since  $T_e$  is time-dependent in these measurements, the coupling rate is also time-dependent. This is depicted in Fig. 6 for the highest fluence using the best fit value of  $\gamma_e^0$ . The 95 K value for the coupling rate,  $\gamma_e(95) = 50 \text{ GHz}$ , is lower than the value  $\gamma_e = 145 \text{ GHz}$ , obtained using a temperature independent analysis with the same physical constants [21]. Within the errors quoted the same value of  $\gamma_e^0$  was found for all fluences. Thus the excitation dependence of the CO response is well accounted for by the dynamical charge transfer model.

The error bars are derived from nonlinear least squares fitting of the the data. However the value of  $\gamma_e^0$  is subject to the uncertainty of two physical parameters encountered in the full fitting procedure. As has been discussed previously, the range of experimental values for the electron-phonon coupling constant affects the value of  $\gamma_e^0$  [6]. In the present analysis an intermediate value of  $G = 0.7 \text{ W/m}^3 \text{ K}$  has been used. For the values of  $G$  at the ends of the experimental range ( $G = 0.3\text{--}1.0 \text{ W/m}^3 \text{ K}$ ), we find  $\gamma_e^0 = 10(\text{}_{-2}^{+6}) \text{ GHz}$  and  $\gamma_e^0 = 30(\pm 7) \text{ GHz}$  respectively. The zero temperature rate  $\gamma_e^0$  also depends on  $\hbar\Omega$  and for the values at the ends of the range  $\hbar\Omega = 30\text{--}60 \text{ cm}^{-1}$ , we

find  $\gamma_e^0 = 21(\pm 7) \text{ GHz}$  and  $\gamma_e^0 = 33(\pm 7) \text{ GHz}$  respectively. As noted above, we are assuming the coupled mode is harmonic. No experimental information yet exists to test this assumption.

The present analysis represents an advance over previous approaches through the use of temperature-dependent coupling rates ( $\gamma_e(T_e)$ ) derived from the dynamical charge transfer model for adsorbate/substrate vibrational energy relaxation. The present fits have similar  $\chi^2$  values to those obtained using the previous method that employed a fixed temperature-independent rate,  $\gamma_e$ . Thus one can see that these experiments do not uniquely establish the presence of temperature dependent rates but the results are entirely consistent with the more complete and basic theoretical model.

#### 4. Conclusion

The dynamical charge transfer model for energy exchange between adsorbate vibrations and substrate electrons involves a coupling rate which is strongly temperature-dependent in two temperature regimes relevant to current femtosecond photoprocess studies. For low frequency adsorbate modes even liquid nitrogen temperatures are sufficient to cause temperature-dependent rates. Electron-hole pair relaxation of adsorbate vibrations can only be considered temperature independent for high frequency modes for which thermal temperatures in the system are much lower than  $\hbar\Omega$ . For femtosecond photoprocess, the electron temperatures are often several thousand degrees. This is high by comparison with the energies of most adsorbate vibrations and thus the temperature dependence of coupling rates will need to be accounted for in models of most femtosecond surface photochemistry.

#### Acknowledgement

It is a pleasure to acknowledge useful conversations with Paul Soven. This work has been supported by the NSF MRL program through Grant # DMR-9120668. AGY acknowledges partial support from the NSF through the PYI Program, and from the Alfred P. Sloan Foundation. RMH acknowledges partial support through grants from the NIH and the NSF.

## References

- [1] J.A. Misewich, A. Kalamarides, T. F. Heinz, U. Hofer and M.M.T. Loy, *J. Chem. Phys.* 100 (1994) 736.
- [2] J.A. Misewich, T.F. Heinz and D.M. Newns, *Phys. Rev. Letters* 68 (1992) 3737.
- [3] J. Prybyla, H. Tom and G. Aumiller, *Phys. Rev. Letters* 68 (1992) 503.
- [4] J.P. Culver, M. Li, L.G. Jahn, R.M. Hochstrasser and A.G. Yodh, *Chem. Phys. Letters* 214 (1993) 431; in: *Laser spectroscopy and photochemistry on metal surfaces*, eds. H.-L. Dai and W. Ho (World Scientific, Singapore), in press.
- [5] T.A. Germer, J.C. Stephenson, E.J. Heilweil and R.R. Cavanagh, *J. Chem. Phys.* 98 (1993) 9986.
- [6] T.A. Germer, J.C. Stephenson, E.J. Heilweil and R.R. Cavanagh, *Phys. Rev. Letters* 71 (1993) 3327; *J. Chem. Phys.* 101 (1994) 1704.
- [7] J.D. Beckerle, M.P. Casassa, R.R. Cavanaugh, E.J. Heilweil and J.C. Stephenson, *Phys. Rev. Letters* 64 (1990) 2090; J.D. Beckerle, M.P. Casassa, E.J. Heilweil, R.R. Cavanaugh and J.C. Stephenson, *J. Electron Spectry.* 54/55 (1990) 17.
- [8] A.L. Harris, N.J. Levinos, L. Rothberg, L.H. Dubois, L. Dhar, S.F. Shane and M.J. Morin, *J. Electron Spectry.* 54/55 (1990) 5; A.L. Harris, L. Rothberg, L. Dhar, N.J. Levinos and L.H. Dubois, *J. Chem. Phys.* 94 (1991) 2438; M. Morin, N.J. Levinos and A.L. Harris, *J. Chem. Phys.* 96 (1992) 3950.
- [9] F.J. Kao, D.G. Bush, D.G. Dacosta and W. Ho, *Phys. Rev. Letters* 70 (1993) 4098.
- [10] F.J. Kao, D.G. Bush, D. Cohen, D.G. Dacosta and W. Ho, *Phys. Rev. Letters* 71 (1993) 2094.
- [11] F. Budde, T.F. Heinz, M.M.T. Loy, J.A. Misewich, F. deRougemont and H. Zacharias, *Phys. Rev. Letters* 66 (1991) 3024.
- [12] F. Budde, T.F. Heinz, A. Kalamarides, M.M.T. Loy and J.A. Misewich, *Surface Sci.* 283 (1993) 143.
- [13] B.N.J. Persson and M. Persson, *Solid State Commun.* 36 (1980) 175.
- [14] M. Head-Gordon and J.C. Tully, *J. Chem. Phys.* 96 (1992) 3939.
- [15] M. Brandbyge, P. Hedegard, T.F. Heinz, J.A. Misewich and D.M. Newns, to be published.
- [16] J.C. Tully, M. Gomez and M. Head-Gordon, *J. Vac. Sci. Technol.* A11 (1993) 1914.
- [17] W.W. Fann, R. Storz, H.W.K. Tom and J. Bokor, *Phys. Rev. Letters* 68 (1992) 2834.
- [18] C.A. Shmittenmaer, M. Aeschlimann, H.E. Elsayed-Ali, R.J.D. Miller, D.A. Mantell, J. Cao and Y. Gao, *Phys. Rev. B* 50 (1995) 8957.
- [19] S.I. Anisimov, B.L. Kapeliovich and T.L. Perel'man, *Zh. Eksp. Teor. Fiz.* 66 (1974) 776.
- [20] H.E. Elsayed-Ali, T. Norris, M.A. Pessot and G. Mourou, *Phys. Rev. Letters* 58 (1987) 1212.
- [21] The following physical constants were used: electron–phonon coupling  $G = 0.7 \times 10^{17}$  W/m<sup>3</sup> K, phonon heat capacity  $C_l = 2.26 \times 10^6$  J/m<sup>3</sup> K, electron heat capacity  $C_e = 96.6T_e$  J/m<sup>3</sup> K<sup>2</sup>, electron diffusion constant  $\kappa = 435(T_e/T_l)$  W/mK.
- [22] K. Wynne and R.M. Hochstrasser, *Chem. Phys.* 193 (1995) 211.
- [23] P. Avouris and R.E. Walkup, *Annu. Rev. Phys. Chem.* 40 (1989) 173.
- [24] T. Hertel, E.Knoesel, E. Hasselbrink, M. Wolf and G.Ertl, *Surface Sci. Letters* 317 (1994) 11147; E. Knoesel, T. Hertel, M. Wolf and G. Ertl, *Chem. Phys. Letters* 240 (1995) 409.
- [25] T.T. Rantala and A. Rosen, *Phys. Rev. B* 34 (1986) 837.
- [26] M. Persson and B. Hellsing, *Phys. Rev. Letters* 49 (1981) 662.
- [27] C. Springer, M. Head-Gordon and J.C. Tully, *Surface Sci.* 320 (1994) L57.
- [28] C.B. Harris, R.M. Shelby and P.A. Cornelius, *Phys. Rev. Letters* 38 (1977) 1415; R.M. Shelby, C.B. Harris and P. Cornelius, *J. Chem. Phys.* 70 (1974) 34; S. Marks, P.A. Cornelius and C.B. Harris, *J. Chem. Phys.* 73 (1980) 3069.
- [29] B.N.J. Persson and R. Ryberg, *Phys. Rev. B* 32 (1985) 3586.
- [30] A.M. Lahee, J.P. Toennies and C. Woll, *Surface Sci.* 177 (1986) 371.